separations

MDPI

Article

UPLC-Q-Orbitrap-MS/MS for Rapid Characterization of the Chemical Constituents of *Atractylodis lancea* and *Atractylodis macrocephalae*

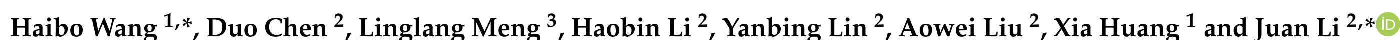

Haibo Wang [1,*], Duo Chen [2], Linglang Meng [3], Haobin Li [2], Yanbing Lin [2], Aowei Liu [2], Xia Huang [1] and Juan Li [2,*]

[1] NMPA Key Laboratory for Quality Control of Traditional Chinese Medicine (Chinese Materia Medica and Prepared Slices), Henan Institute for Drug and Medical Device Control (Henan Vaccine Issuance Center), Zhengzhou 450018, China; 18595506180@163.com
[2] Key Laboratory of Advanced Drug Preparation Technologies, Ministry of Education, School of Pharmaceutical Sciences, Zhengzhou University, Zhengzhou 450001, China; linyb1357@163.com (Y.L.)
[3] College of Agriculture, Shihezi University, Shihezi 832003, China; 18037110402@163.com
* Correspondence: haibowang99@163.com (H.W.); jli@zzu.edu.cn (J.L.)

Abstract

Atractylodis lancea (Cangzhu) and *Atractylodes macrocephala* (Baizhu) are two traditional Chinese medicines with complex chemical compositions. However, a comprehensive comparative analysis of their constituents remains lacking. In this work, an ultra-high-performance liquid chromatography coupled with quadrupole-Orbitrap tandem mass spectrometry (UPLC-Q-Orbitrap-MS/MS) method was developed for the rapid characterization and differentiation of chemical components in Cangzhu and Baizhu. Chromatographic separation was achieved on a C18 column with gradient elution, and compounds were detected using electrospray ionization in both positive and negative modes. By analyzing characteristic fragmentation patterns and neutral losses, a total of 111 compounds were tentatively identified, including 14 common components (present in both species) and 97 differential components (unique to one species). This study presents the first comprehensive comparative chemical profiling of the two *Atractylodes* species, offering valuable references for pharmacodynamic material basis studies and quality control.

Keywords: UPLC-Q-Orbitrap-MS/MS; *Atractylodis lancea*; *Atractylodes macrocephala*; chemical components; identification

Check for updates

Academic Editor: Didier Thiébaut

Received: 11 April 2026
Revised: 12 May 2026
Accepted: 25 May 2026
Published: 29 May 2026

Copyright: © 2026 by the authors. Licensee MDPI, Basel, Switzerland. This article is an open access article distributed under the terms and conditions of the Creative Commons Attribution (CC BY) license.

1. Introduction

Atractylodis lancea (Cangzhu) and *Atractylodis Macrocephalae* (Baizhu), both of which belong to the Asteraceae family, have a long history of medicinal use in China [1]. Cangzhu is derived from the dried rhizomes of *Atractylodes lancea* (Thunb.) DC and is known for its effects in eliminating dampness, invigorating the spleen, dispelling wind and cold, and improving eyesight [1,2]. Baizhu is derived from the dried rhizome of *Atractylodes macrocephala* Koidz and effectively invigorates the spleen, replenishes *qi*, eliminates dampness, promotes diuresis, checks sweating, and prevents miscarriage [1,3]. Consequently, the two herbs are not interchangeable in clinical practice, and differences in their chemical composition account for their distinct therapeutic effects [4–6].

Traditional Chinese medicines are chemically complex, and their components constitute the material basis for their pharmacological activities. Liquid chromatography coupled with tandem mass spectrometry (LC-MS/MS) has emerged as a powerful tool for

 https://doi.org/10.3390/separations13060164

characterizing TCM components due to its high sensitivity, high resolution, and ability to profile complex mixtures without extensive isolation [7–10]. Several studies have applied LC-MS/MS to analyze *Atractylodes* species. Xu et al. [11] employed UHPLC-Q-TOF-MS/MS to rapidly detect and identify the components in Baizhu *Shaoyao San* (BSS); a total of 186 compounds were ultimately identified in crude and processed BSS, among which 62 marker compounds showing significant differences between the two forms were identified using principal component analysis and *t*-tests. Zhou et al. [12] used UPLC-Q-TOF-MS/MS to rapidly analyze the chemical components of *Atractylodes lancea* (Thunb.) DC. and *Atractylodes chinensis* (DC.) Koidz., identifying 78 chemical components, including 16 terpenoids, 10 polyacetylenes, 25 organic acids, 17 glycosides, and 10 other compounds. Yang et al. [13] employed UPLC-Q-TOF-MS^E to analyze the chemical components of *Atractylodes macrocephala* from three different origins; a total of 53 chemical components were identified, and 21 differential components were characterized through multivariate statistical analysis, including 18 common differential components and three unique components. However, a direct and comprehensive comparative analysis of the chemical constituents between Cangzhu and Baizhu under identical analytical conditions remains lacking. Such a comparison is essential for elucidating the chemical basis of their different pharmacological effects and for establishing species-specific quality control markers.

In this study, we developed a UPLC-Q-Orbitrap-MS/MS method for the rapid simultaneous characterization of chemical constituents in Cangzhu and Baizhu. Using 70% methanol extracts, components were identified based on retention times, accurate masses, and MS/MS fragment patterns, and the Compound Discovery (CD) database. The main objectives were: (1) to establish a reliable analytical method for comprehensive profiling of the two herbs; (2) to identify common and differential components between them; and (3) to summarize the fragmentation behaviors of major compound classes (terpenoids, coumarins, flavonoids, phenylpropanoids, alkaloids, and amino acids). This work provides a comparative chemical inventory that supports future pharmacodynamic studies and quality control of different *Atractylodes* varieties.

2. Materials and Methods

2.1. Chemicals and Materials

HPLC grade methanol and acetonitrile were purchased from Thermo Fisher Scientific Corporation (Milford, MA, USA). Formic acid and acetic acid were purchased from DIKMA (Milford, MA, USA). Ultra-pure water was prepared by a Milli-Q ultra-pure water preparation system (Merck, Darmstadt, Germany). Cangzhu and Baizhu were purchased from Zhang Zhongjing Pharmacy (Zhengzhou, China) and authenticated by Professor Chengxue Pan (Department of Chinese Materia Medica, School of Pharmaceutical Sciences, Zhengzhou University). All voucher specimens were deposited in our laboratory.

2.2. Sample Preparation

Dried Cangzhu and Baizhu were ground into powder and passed through a 40-mesh sieve. One gram of the powder was accurately weighed and placed in a 50 mL flask. Then, 20 mL of 70% methanol–water (*v*/*v*) was added, and the mixture was ultrasonicated in a water bath (power: 250 W; frequency: 40 kHz) for 60 min. After ultrasonication, the extract was cooled to room temperature. The flask was then reweighed, and the lost mass was supplemented with 70% methanol–water. The solution was shaken well and centrifuged at 12,000 rpm for 10 min. The supernatant was collected and filtered through a 0.22 μm microporous membrane to obtain the sample solution for UPLC-Q-Orbitrap-MS analysis.

https://doi.org/10.3390/separations13060164

2.3. Instrumentation Conditions

The present study was performed on an Ultimate 3000UPLC system coupled with Orbitrap Exploris mass spectrometer equipped with an electrospray ionization (ESI) source (Thermo Fisher Scientific). Chromatographic separation was achieved on Waters Xbridge C18 column (2.1 × 100 mm, 1.7 μm) maintained at 35°C. The mobile phases consisted of H_2O containing 0.1% formic acid (phase A) and methanol (phase B). The phases were delivered at a flow rate of 0.25 mL/min using a linear gradient program as follows: 0–3 min, 10–40% B; 3–8 min, 40–80% B; 8–12 min, 80–100% B; 12–16 min, 100–100% B; 16–20 min, 100–10% B; and 20–27 min, 10% B. The injection volume was 2 μL.

High-resolution mass spectrometry data were acquired in ESI modes. In the full-scan mass spectra, most of the authentic compounds exhibited $[M+H]^+$ ions in positive ion mode or $[M-H]^-$ ions in negative ion mode. A full MS/dd-MS^2 (TopN) scan method was applied to the samples. The source parameters were as follows: spray voltage: 3.4 kV (positive) or −2.5 kV (negative); ion transfer tube temperature: 320 °C; vaporizer temperature: 350 °C; sheath gas: 50 arb; and auxiliary gas: 10 arb. The Orbitrap analyzer scanned over m/z 70–1000 Da at a resolution of 120,000 FWHM in Full-MS mode. Data-dependent MS^2 scans were performed at a resolution of 60,000 FWHM, with four scans per cycle. MS^2 fragmentation was carried out using higher-energy collisional dissociation (HCD) with stepped normalized collision energies of 10%, 20%, 30%, and 40%, and an isolation width of 2.0 Da. The five most intensive precursor ions were automatically selected for MS^2 fragmentation. A dynamic exclusion time of 6 s was set to record the fragmentation information of minor compounds in cases of co-elution. Data acquisition and processing were performed using Xcalibur Qual Browser software (Thermo Fisher Scientific, Waltham, MA, USA).

2.4. Data Acquisition and Analysis

Mass spectrometry data acquisition was performed using Xcalibur software 4.1 (Qual Browser module), while subsequent processing and analysis were conducted with Compound Discovery (CD) software 3.1. In positive ion mode, quasi-molecular ions were detected as $[M+H]^+$. In negative ion mode, quasi-molecular ions were detected as $[M-H]^-$. Compound identification was performed by integrating multiple lines of evidence, including retention times, accurate MS^1 and MS/MS data, fragmentation patterns, and comparisons with online databases.

3. Results and Discussion

3.1. Optimization of Chromatographic and Mass Spectrometric Conditions

To achieve satisfactory separation and high responses for most components in Cangzhu and Baizhu, key chromatographic parameters were systematically optimized. The optimal chromatographic conditions were as follows: column temperature, 35 °C; flow rate, 0.25 mL/min; and the mobile phase of methanol and water (containing 0.1% formic acid) under gradient elution, which demonstrated good peak distributions and high signal intensities.

Given the chemical complexity of the two herbal matrices, both positive and negative ion modes were employed to obtain comprehensive spectral information. Optimization of collision energy (CE) at normalized values of 10%, 20%, 30%, and 40% showed that 30% CE yielded the most informative fragments for structural identification. Other MS parameters, such as ion transfer tube temperature, vaporizer temperature, sheath gas, and auxiliary gas, were further tuned to maximize signal-to-noise ratios for low-abundance compounds. These optimized conditions ensured reproducible and discriminative profiling for subsequent analysis.

3.2. Qualitative Analysis of Compounds in Cangzhu and Baizhu

The optimized UPLC/Q-Orbitrap MS/MS method was applied to analyze the 70% methanol extracts of Cangzhu and Baizhu in positive and negative ion modes. The identification procedure consists of four sequential steps: (1) peak detection using Compound Discoverer software from UPLC-Q-Orbitrap-MS/MS data (retention time, accurate mass ≤5 ppm, and MS/MS fragments); (2) database matching against mzCloud, ChemSpider, and local TCM databases; (3) manual confirmation by comparing fragmentation patterns and neutral losses; and (4) classification into common components (present in both species) or differential components (unique to one species). A total of 125 components were identified in Cangzhu and Baizhu by matching with the CD software database and with the assistance of published studies [11,14]. Among these, 14 common components and 97 differential components were identified. These differential components can serve as a basis for distinguishing between the two varieties. The total ion chromatograms of *Cangzu* and *Baizu* in positive and negative ion modes are shown in Figure 1. Detailed information for the identified peaks, including retention times, molecular formulas, ion types, detected masses, mass errors, fragment ions, and sources, is summarized in Table S1. As shown in Figure 1A–D, the total ion chromatograms of Cangzhu and Baizhu exhibited distinct profiles in terms of peak intensity and distribution, indicating differences in their chemical composition. The main mass spectrometry information and retention times of representative components are provided in Table 1.

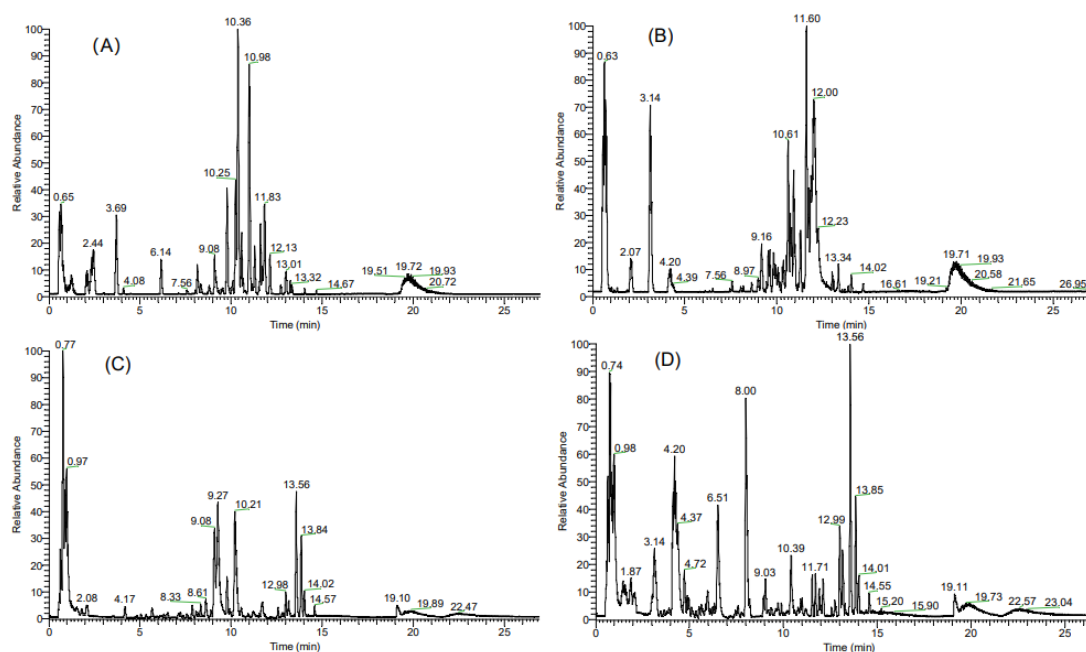

Figure 1. Total ion chromatograms of *Cangzu* and *Baizu* extracts in positive ion mode (**A**,**B**) and in negative ion mode (**C**,**D**).

Table 1. Main mass spectrometry information and retention times of representative components.

Compound	T_R (min)	Molecular Formula	Detected Mass (*m/z*)	Ion Type	Mass Error (ppm)	Fragment Ions (*m/z*)
Caryophyllene oxide	9.92	$C_{15}H_{24}O$	221.18964	$[M+H]^+$	−3.88	203.17807, 147.11588, 133.10028
Turmerone	5.33	$C_{15}H_{20}O$	217.15829	$[M+H]^+$	−4.17	199.14670, 161.09502, 107.08479
Artemisinin	9.24	$C_{15}H_{22}O_5$	283.15325	$[M+H]^+$	−4.43	237.14709, 219.13667, 191.14189
1α-hydroxy-1-desoxotamirin	8.04	$C_{15}H_{20}O_4$	265.14308	$[M+H]^+$	−3.48	247.13148, 229.12100, 205.12114
Camphor	5.87	$C_{10}H_{16}O$	153.12731	$[M+H]^+$	−3.87	135.11592, 109.10046, 43.05394
Rosiridin	5.70	$C_{16}H_{28}O_7$	333.19031	$[M+H]^+$	−2.96	279.15726, 135.11592, 85.02778

Table 1. *Cont.*

Compound	T_R (min)	Molecular Formula	Detected Mass (*m*/*z*)	Ion Type	Mass Error (ppm)	Fragment Ions (*m*/*z*)
Furopinnarin	9.99	$C_{17}H_{16}O_4$	285.11168	$[M+H]^+$	−3.59	225.08954, 165.06879
7-hydroxy-6-methoxy-2H-chromen-2-one	4.25	$C_{10}H_8O_4$	193.04954	$[M+H]^+$	−2.91	133.02750
Marmesin	6.51	$C_{14}H_{14}O_4$	247.09588	$[M+H]^+$	−4.55	229.08438, 201.08969
Iristectorin B	6.67	$C_{23}H_{24}O_{12}$	493.13276	$[M+H]^+$	−3.74	331.07892, 85.02783
4-Methoxycinnamaldehyde	6.27	$C_{10}H_{10}O_2$	163.07538	$[M+H]^+$	−3.2	131.04823, 103.05423
4-methoxy-6-(prop-2-en-1-yl)-2H-1,3-benzodioxole	8.79	$C_{11}H_{12}O_3$	193.08560	$[M+H]^+$	−4.68	165.08997, 133.06400
Arginine	0.68	$C_6H_{14}N_4O_2$	175.11894	$[M+H]^+$	−3.17	116.06982, 60.05523
Isoleucine	1.19	$C_6H_{13}NO_2$	132.10216	$[M+H]^+$	−2.61	87.09922, 86.09586
Aspartic acid	0.75	$C_4H_7NO_4$	134.04494	$[M+H]^+$	−2.68	87.05478
Lauric acid	12.12	$C_{12}H_{24}O_2$	199.16799	$[M-H]^-$	−4.99	152.91064, 106.91794, 61.98804
Lactic acid	0.93	$C_3H_6O_3$	89.02347	$[M-H]^-$	−4.84	71.01348, 59.01353
Atropine	8.82	$C_{17}H_{23}NO_3$	290.17456	$[M+H]^+$	−3.57	244.16797, 231.13638, 213.12598
Laudanosine	8.94	$C_{21}H_{27}NO_4$	358.20068	$[M+H]^+$	−3.12	342.16271, 298.17831, 84.08028

3.2.1. Characterization of Terpenoids

A total of 13 terpenoids, including monoterpenoids, sesquiterpenoids, and diterpenoids were characterized and identified. Due to structural differences, the fragmentation pathways of monoterpenoids, sesquiterpenoids, and diterpenoids varied slightly. The parent ion $[M+H]^+$ of compound **1** was observed at *m*/*z* 221.18964, and the molecular formula was $C_{15}H_{24}O$. It was identified as caryophyllene oxide based on the CD database [15]. The neutral loss of H_2O from *m*/*z* 221.18964 yielded the product ion at *m*/*z* 203.17807, and subsequent loss of a C_4H_8 group from this ion produced the fragment ion at *m*/*z* 147.11588. Compound **2** showed a parent ion $[M+H]^+$ at *m*/*z* 217.15829, with the molecular formula $C_{15}H_{20}O$. It was identified as turmerone according to the CD database [16]. The neutral loss of H_2O and C_4H_8 from the precursor ion at *m*/*z* 217.15829 yielded the product ions at *m*/*z* 199.14670 and *m*/*z* 161.09502, respectively. Subsequent loss of a C_7H_8 group from the ion at *m*/*z* 199.14670 gave the fragment ions at *m*/*z* 107.08479.

Compound **3** exhibited the parent ion $[M+H]^+$ at *m*/*z* 283.15325, corresponding to the molecular formula $C_{15}H_{22}O_5$. It was identified as artemisinin based on the CD database [17]. The neutral loss of HCOOH from the precursor ion at *m*/*z* 283.15325 yielded a product ion at *m*/*z* 237.14709, while loss of H_2O produced the fragment ion at *m*/*z* 219.13667. Subsequent loss of CO_2 produced the fragment ion at *m*/*z* 191.14189. Compound **6** showed the parent ion $[M+H]^+$ at *m*/*z* 265.14308, with the molecular formula $C_{15}H_{20}O_4$. It was identified as 1α-hydroxy-1-desoxotamirin according to the CD database [18]. The neutral loss of H_2O from the precursor ion at *m*/*z* 265.14308 yielded a product ion at *m*/*z* 247.13148, and subsequent loss of CO_2 and H_2O produced the fragment ions at *m*/*z* 205.12114 and *m*/*z* 229.12100, respectively. The parent ion $[M+H]^+$ of compound **10** was observed at *m*/*z* 153.12731, and the molecular formula was $C_{10}H_{16}O$. Compound **10** was identified as camphor according to the CD database [19]. The neutral loss of H_2O from the precursor ion at *m*/*z* 153.12731 yielded the product ion at *m*/*z* 135.11592. Additionally, losses of C_2H_4O and C_8H_{14} from the precursor ion produced the fragment ions at *m*/*z* 109.10046 and *m*/*z* 43.05394, respectively. Compound **13** showed a parent ion $[M+H]^+$ at *m*/*z* 333.19031, with the molecular formula $C_{16}H_{28}O_7$. It was identified as rosiridin following the CD database [20]. The loss of three H_2O molecules from the precursor ion at *m*/*z* 333.19031 yielded a product ion at *m*/*z* 279.15726. Subsequent O-glycosidic bond cleavage and sugar ring breakage from this ion produced fragment ions at *m*/*z* 135.11592 and *m*/*z* 85.02778, respectively. The detailed fragmentation pathways of compounds **1**, **2**, **3**, **6**, **10**, and **13** are shown in Figure 2.

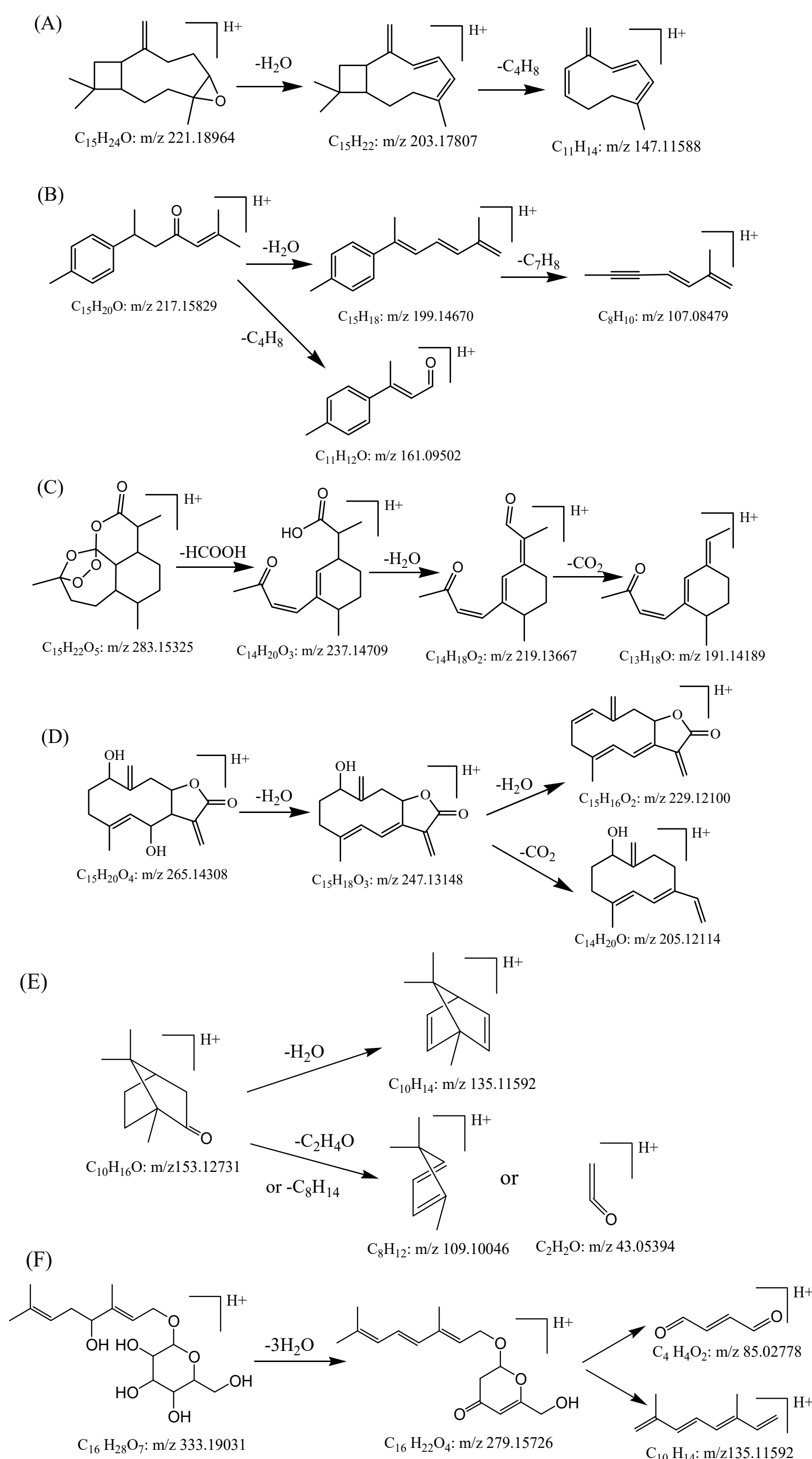

Figure 2. Detailed fragmentation pathways of sesquiterpenes (**A**–**D**) and monoterpenoids (**E**,**F**): (**A**) compound **1** (caryophyllene oxide); (**B**) compound **2** (turmerone); (**C**) compound **3** (artemisinin); (**D**) compound **6** (1α-hydroxy-1-desoxotamirin); (**E**) compound **10** (camphor); and (**F**) compound **13** (rosiridin).

3.2.2. Characterization of Coumarins and Flavonoids

Five coumarins and two flavonoids were characterized and identified in Cangzhu and Baizhu. The parent ion $[M+H]^+$ of compound **14** was observed at m/z 285.11168. Its molecular formula was $C_{17}H_{16}O_4$, with a mass error of −3.59 parts per million (ppm). Compound **14** was identified as furopinnarin based on the CD database [21]. The neutral

loss of CH_4 and CO_2 from the precursor ion at m/z 285.11168 yielded the product ion at m/z 225.08954. The parent ion $[M+H]^+$ of compound **15** was observed at m/z 193.04954, and its molecular formula was $C_{10}H_8O_4$. Compound **15** was identified as 7-hydroxy-6-methoxy-2H-chromen-2-one based on the CD database [22]. The neutral loss of CH_4 and CO_2 from the precursor ion at m/z 193.04954 yielded a product ion at m/z 133.02750. The parent ion $[M+H]^+$ of compound **16** was observed at m/z 247.09588. Its molecular formula was $C_{14}H_{14}O_4$, with a mass error of −4.55 ppm. Compound **16** was identified as marmesin based on the CD database [23]. The neutral loss of H_2O and CO_2 from the precursor ion at m/z 247.09588 yielded the product ions at m/z 229.08438 and m/z 201.08969, respectively. The parent ion $[M+H]^+$ of compound **19** was observed at m/z 493.13276, and the molecular formula was $C_{23}H_{24}O_{12}$. Compound **19** was identified as iristectorin B based on the CD database [24]. Cleavage of the O-glycosidic bond and neutral loss of $C_6H_{10}O_5$ from the precursor ion at m/z 493.13276 yielded the product ion at m/z 331.07892. The detailed fragmentation pathways of compounds **14**, **15**, **16**, and **19** are shown in Figure 3.

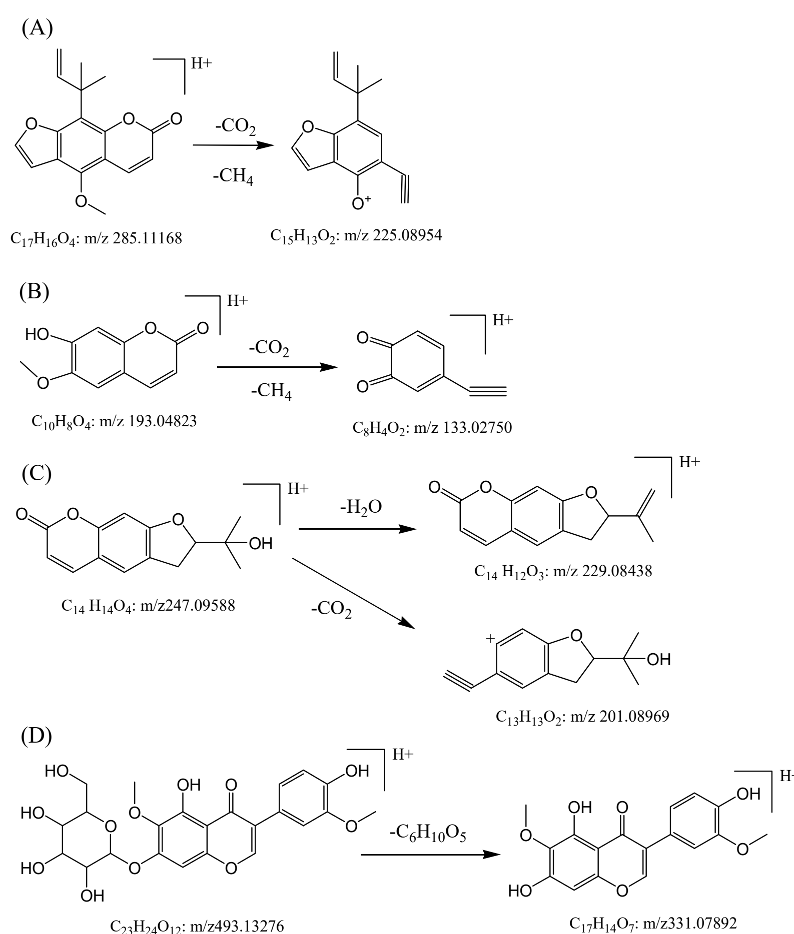

Figure 3. Detailed fragmentation pathways of coumarins and flavonoids: (**A**) compound **14** (furopinnarin), (**B**) compound **15** (7-hydroxy-6-methoxy-2H-chromen-2-one), (**C**) compound **16** (marmesin), and (**D**) compound **19** (iristectorin B).

3.2.3. Characterization of Phenylpropanoids and Alkaloids

Four phenylpropanoids and six alkaloids were characterized and identified in Cangzhu and Baizhu. The parent ion $[M+H]^+$ of compound **21** was observed at m/z 163.07538. Its molecular formula was $C_{10}H_{10}O_2$, with a mass error of 3.20 ppm. Compound **21** was identified as 4-methoxycinnamaldehyde based on the CD database [25]. The neutral loss of CH_3OH from the precursor ion at m/z 163.07538 yielded the product ion at m/z 131.04823, and subsequent loss of CO produced the fragment ion at m/z 103.05423.

The parent ion $[M+H]^+$ of compound **22** was observed at m/z 193.08560, and the molecular formula was $C_{11}H_{12}O_3$. Compound **22** was identified as 4-methoxy-6-(prop-2-en-1-yl)-2H-1,3-benzodioxole [26]. The neutral loss of CO from the precursor ion at m/z 193.08560 yielded a product ion at m/z 165.08997, and subsequent loss of CH_3OH from m/z 165.08997 produced the fragment ion at m/z 133.06400. The parent ion $[M+H]^+$ of compound **88** was observed at m/z 290.17456. The molecular formula was $C_{17}H_{23}NO_3$, with a mass error of −3.57 ppm. The neutral loss of CH_4 and HCOH from the precursor ion at m/z 290.17456 yielded a product ion at m/z 244.16797. Compound **88** was identified as atropine [27]. The parent ion $[M+H]^+$ of compound **92** was observed at m/z 358.20068, and the molecular formula was $C_{21}H_{27}NO_4$. The neutral loss of CH_4 and $4CH_3$ from the precursor ion yielded the product ions at m/z 342.16271 and m/z 298.17831, respectively. Compound **92** was identified as laudanosine according to the CD database [28]. The detailed fragmentation pathways of compounds **21**, **22**, **88**, and **92** are shown in Figure 4.

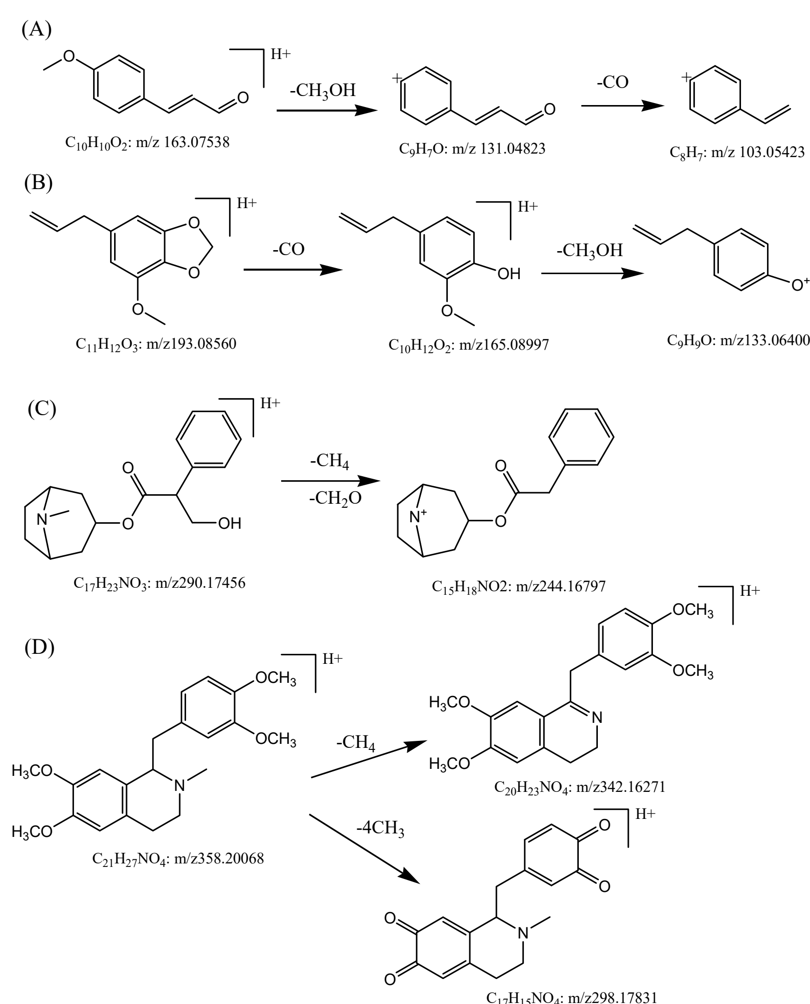

Figure 4. Detailed fragmentation pathways of phenylpropanoids and alkaloids: (**A**) compound **21** (4-Methoxycinnamaldehyde), (**B**) compound **22** (myristicin), (**C**) compound **88** (atropine), and (**D**) compound **92** (laudanosine).

3.2.4. Characterization of Amino Acids, Organic Acids, and Fatty Acids

Amino acids are common components found in animals and plants; thus, almost every TCM contains this type of compound, which can be detected in the form of $[M+H]^+$. The fragmentation of these components mainly involves the neutral loss of HCOOH (46.01 Da) and NH_3 (17.02 Da). Finally, eighteen amino acids, six organic acids and twenty-six fatty acids were detected in the extracts of Cangzhu and Baizhu. For example, arginine,

https://doi.org/10.3390/separations13060164

isoleucine, and aspartic acid generated fragment ions at *m/z* 116.06982, 86.09586, and 97.05478, respectively, through the loss of guanidine (CH_5N_3) and HCOOH. Therefore, compounds **25**, **26**, **27**, **28**, **29**, **30**, **31**, **32**, and **33** could be rapidly identified as amino acids [29]. In addition, organic acids and fatty acids are predominantly detected in negative ion mode as $[M-H]^-$ ions. According to the loss of HCOOH (46.00 Da) and CO_2 (44.00 Da) from side-chain groups, compounds **70** and **44** were identified as lactic acid and lauric acid [30,31], respectively. The detailed fragmentation pathways of compounds **25**, **26**, **32**, **70**, and **44** are shown in Figure 5.

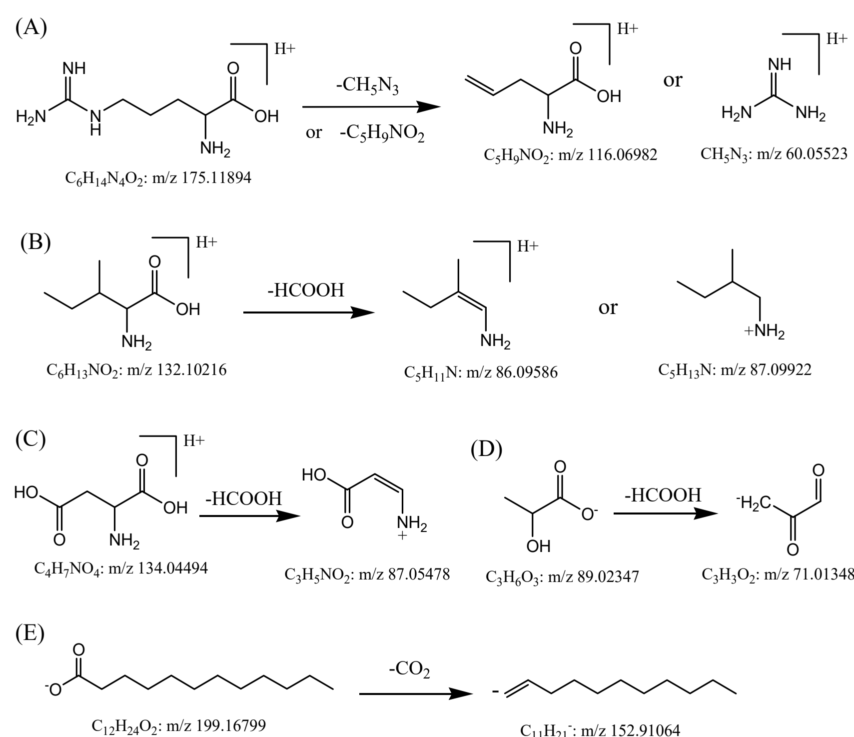

Figure 5. Detailed fragmentation pathways of amino acids and fatty acids: (**A**) compound **25** (arginine), (**B**) compound **26** (isoleucine), (**C**) compound **32** (aspartic acid), (**D**) compound **70** (lactic acid), (**E**) compound **44** (lauric acid).

4. Conclusions

In this study, a UHPLC-Q-Orbitrap-MS/MS method was established for the rapid simultaneous characterization of chemical constituents in Cangzhu and Baizhu. A total of 125 compounds were identified or tentatively characterized, covering terpenoids, coumarins, flavonoids, phenylpropanoids, alkaloids, organic acids, amino acids, and fatty acids. Among the identified compounds, 14 were present in both species, while 97 were differential components unique to either Cangzhu or Baizhu. These differential components can serve as potential chemical markers for quality control and species authentication. However, a limitation of this method is the difficulty in distinguishing certain isomeric compounds, which may require reference standards or NMR analysis for unambiguous identification. Despite this limitation, the present study provides a comprehensive and comparative chemical inventory of the two *Atractylodes* species, thereby supporting further investigation into their differential pharmacodynamics and quality evaluation.

Supplementary Materials: The following supporting information can be downloaded at: https://www.mdpi.com/article/10.3390/separations13060164/s1. Table S1: Details of the identified peaks, such as retention times, molecular formulas, ion types, detected masses, mass errors, fragment ions, and sources.

Author Contributions: Conceptualization, H.W. and J.L.; Methodology, D.C.; Validation, D.C., H.L. and Y.L.; Formal Analysis, L.M., A.L. and X.H.; Investigation, D.C. and H.L.; Data Curation, L.M., Y.L., A.L. and X.H.; Writing—Original Draft, J.L.; Writing—Review and Editing, H.W. and J.L.; Visualization, D.C. and L.M.; Project Administration, H.W. and J.L.; Funding Acquisition, H.W. All authors have read and agreed to the published version of the manuscript.

Funding: This work was supported by the Key Research and Development Projects of Henan Province (No. 231111312700), the National Key Research and Development Program of China (No. 2024YFC3607500), and Open Project of NMPA Key Laboratory for Quality Control of Traditional Chinese Medicine (Chinese Materia Medica and Prepared Slices) (No. KF202405).

Data Availability Statement: The original contributions presented in this study are included in the article and Supplementary Material. Further inquiries can be directed to the corresponding authors.

Conflicts of Interest: The authors declare no conflicts of interest.

References

1. Editorial Committee of Chinese Pharmacopoeia. *Pharmacopoeia of the People's Republic of China*; China Medical Science and Technology Press: Beijing, China, 2020; Volume 1, pp. 107–168.
2. Li, K.D.; Cao, Z.j.; Ao, H. Research Progress on Chemical Components and Pharmacological Effects of Atractylodes. *J. Chengdu Univ. Tradit. Chin. Med.* **2024**, *47*, 73–80. [CrossRef]
3. Yang, D.Y.; Yu, H.; Wu, X.Y.; Zhu, Y.H.; Xiao, X.L.; Xu, W.N.; Chen, Y.X.; Gong, Q.F. Research Progress on Chemical Constituents and Their Biological Activities of Baizhu (*Atractylodis macrocephala*). *Chin. Arch. Tradit. Chin. Med.* **2023**, *41*, 171–182.
4. Shi, K.; Xiao, Y.X.; Dong, Y.; Wang, D.P.; Xie, Y.; Tu, J.Y.; Xu, K.; Zhou, Z.S.; Cao, G.S.; Liu, Y.J. Protective Effects of *Atractylodis lancea* Rhizoma on Lipopolysaccharide-Induced Acute Lung Injury via TLR4/NF-κB and Keap1/Nrf2 Signaling Pathways In Vitro and In Vivo. *Int. J. Mol. Sci.* **2022**, *23*, 16134. [CrossRef]
5. Yang, L.; Yu, H.; Hou, A.; Man, W.J.; Wang, S.; Zhang, J.X.; Wang, X.J.; Zheng, S.W.; Jiang, H.; Kuang, H.X. A review of the ethnopharmacology, phytochemistry, pharmacology, application, quality control, processing, toxicology, and pharmacokinetics of the dried rhizome of *Atractylodes macrocephala*. *Front. Pharmacol.* **2021**, *12*, 727154. [CrossRef]
6. Amin, M.J.; Hossen, X.Q.; Fu, J.Y.; Chou, J.Y.; Wu, X.Q.; Wang, Y.J.; Chen, Y.; Wu, C.L.; Yin, X.B.; Dou, C.; et al. Inhibition of the Akt/NF-κB pathway is involved in the anti-gastritis effects of an ethanolic extract of the rhizome of *Atractylodes macrocephala*. *J. Ethnopharmacol.* **2022**, *293*, 115251. [CrossRef]
7. Huang, M.L.; Yu, S.J.; Shao, Q.; Liu, H.; Wang, Y.C.; Chen, H.Z.; Huang, Y.; Wang, Y. Comprehensive profiling of Lingzhihuang capsule by liquid chromatography coupled with mass spectrometry-based molecular networking and target prediction. *Acupunct. Herbal. Med.* **2022**, *2*, 58–67. [CrossRef]
8. Tang, X.Y.; Zeng, J.X.; Wang, X.X.; Xu, W.Y.; Zhao, P.C.; Fan, C.L.; Yao, Z.H.; Yao, X.S.; Dai, Y. Chemical and metabolic profiling of Codonopsis Radix extract with an integrated strategy using ultra-high- performance liquid chromatography coupled with mass spectrometry. *J. Sep. Sci.* **2023**, *46*, 2200723. [CrossRef] [PubMed]
9. Ding, M.; Wen, J.H.; Guo, Z.F.; Li, M.N.; Wang, G.J.; Li, P.; Yang, H. Comprehensive chemical profiling and quantification of Shexiang Xintongning Tablets by integrating liquid chromatography-mass spectrometry and gas chromatography-mass spectrometry. *ARAB J. Chem.* **2023**, *16*, 104527. [CrossRef]
10. Chen, T.T.; Wang, X.N.; Chen, P.; Zheng, Y.Y.; He, Y.; Zeng, X.; Peng, W.; Su, W.W. Chemical components analysis and in *vivo* metabolite profiling of Jian'er Xiaoshi oral liquid by UHPLC-QTOF-MS/MS. *J. Pharm. Biomed. Anal.* **2022**, *211*, 114629. [CrossRef] [PubMed]
11. Xu, Y.Y.; Cai, H.; Cao, G.; Duan, Y.; Pei, K.; Tu, S.C.; Zhou, J.; Xie, L.; Sun, D.D.; Zhao, J.Y.; et al. Profiling and analysis of multiple constituents in Baizhu Shaoyao San before and after processing by stir-frying using UHPLC/Q-TOF-MS/MS coupled with multivariate statistical analysis. *J. Chromatogr. B* **2018**, *1083*, 110–123. [CrossRef]
12. Zhou, J.; Tang, W.W.; Chen, J. A UPLC-QTOF-MS/MS method for the characterization of chemical constituents of *Atractylodes lancea* (Thunb.) DC. and *Atractylodes chinensis* (DC.) Koidz. *J. Pathol. Clin. Res.* **2020**, *28*, 321–328.
13. Yang, L.; Yu, Y.; Kang, S.Y.; Yan, G.L.; Sun, H.; Wang, X.J. Analysis of chemical constituents and their regional differences of *Atractylodes macrocephala* based on UPLC-MS^E. *Chin. Tradit. Herb. Drugs* **2024**, *55*, 1344–1353.
14. Shu, L.X.; Zhang, S.M.; Qiu, H.X.; Yao, Y.Q.; Liu, S.T.; Qian, J.; Chen, S.Y.; Zhao, Q.D.; Li, Y.B. Rapid classification and identification of chemical components in three different Zanthoxylum species by ultra-high-performance-liquid chromatography quadrupole-orbitrap-mass spectrometry. *J. Sep. Sci.* **2024**, *47*, 2300670. [CrossRef] [PubMed]
15. Gyrdymova, Y.V.; Rubtsova, S.A. Caryophyllene and caryophyllene oxide: A variety of chemical transformations and biological activities. *Chem. Pap.* **2022**, *76*, 1–39. [CrossRef]

16. Yu, J.Y.; Hu, W.J.; Zhang, X.B. Study on the synthesis, structural characterization and antifungal mechanism of ar-turmerone derivatives. *J. Mol. Struct.* **2025**, *1346*, 142821. [CrossRef]
17. Chutvirasakul, B.; Joseph, J.F.; Parr, M.K.; Suntornsuk, L. Development and applications of liquid chromatography-mass spectrometry for simultaneous analysis of anti-malarial drugs in pharmaceutical formulations. *J. Pharm. Biomed. Anal.* **2021**, *195*, 113855. [CrossRef]
18. Todorova, M.; Altantsetseg, S.; Staneva, J.; Shatar, S. Lactone profile of *Brachanthemum gobicum* Krasch from Mongolian gobi. *Proc. Natl. Acad. Sci. USA* **2010**, *63*, 225–228.
19. Hayashi, K.; Kumagai, H.; Sawada, H. Liquid chromatography electrospray ionization mass spectrometry analysis of camphor and menthol. *Chromatography* **2023**, *44*, 33–37. [CrossRef]
20. Schötz, K.; Mattioli, L.; Perfumi, M.; Koch, E. Plasma levels of rosiridin after oral administration of a Rhodiola rosea extracts in rats. *Planta Med.* **2015**, *81*, 1538. [CrossRef]
21. Estévez Reyes, R.; González González, A. Structure of pinnarin and furopinnarin, two new coumarins from the roots of Ruta pinnata. *Phytochemistry* **1970**, *9*, 833–840. [CrossRef]
22. Parasecolo, L.; Monsalvo, I.M.; Kovinich, N.; Ifa, D.R. Development of a Matrix-Assisted Laser Desorption Ionization High Resolution Mass Spectrometry Method for the Quantification of Camalexin and Scopoletin in *Arabidopsis thaliana*. *Rapid Commun. Mass. Spectrom.* **2025**, *39*, e9973. [CrossRef]
23. Wu, W.; Hong, L.; Dai, S.S.; Liang, Y.Q.; Pu, W.L.; Li, K.L.; Zhang, H.Y.; Feng, C.L. Chemical constituents of EtOAc extracts of *Angelica gigas* and anti-prostate carcinoma activities. *Chin. Tradit. Herb. Drugs* **2025**, *56*, 1903–1915.
24. Zhang, Y.Y.; Wang, Q.; Qi, L.W.; Qin, X.Y.; Qin, M.J. Characterization and determination of the major constituents in Belamcandae Rhizoma by HPLC-DAD-ESI-MS^n. *J. Pharm. Biomed. Anal.* **2011**, *56*, 304–314. [CrossRef] [PubMed]
25. Wang, K.C.; Chang, J.S.; Chiang, L.C.; Lin, C.C. 4-Methoxycinnamaldehyde inhibited human respiratory syncytial virus in a human larynx carcinoma cell line. *Phytomedicine* **2009**, *16*, 882–886. [CrossRef] [PubMed]
26. Götz, M.E.; Sachse, B.; Schäfer, B.; Eisenreich, A. Myristicin and Elemicin: Potentially Toxic Alkenylbenzenes in Food. *Foods* **2022**, *11*, 1988. [CrossRef] [PubMed]
27. Qiu, Q.Q.; Lu, Y.; Wang, X.R.; Wu, B.J.; Wang, H.Y.; Sun, J.B. Determination of atropine in cream cosmetics by ultraperformance liquid chromatography-quadrupole/time-of-flight high-resolution mass spectrometry. *China Surfactant Deterg. Cosmet.* **2023**, *53*, 706–713.
28. Cui, X.Z.; Lian, R.; Chen, J.; Ni, C.F.; Liang, C.; Chen, G.L.; Zhang, Y.R. Source identification of heroin by rapid detection of organic impurities using direct analysis in real time with high-resolution mass spectrometry and multivariate statistical analysis. *Microchem. J.* **2019**, *147*, 121–126. [CrossRef]
29. Li, J.; Wang, Q.L.; Liu, Y.; Ke, Y.; Fan, Q.Q.; Zhou, P.; An, M.C.; Liu, H.M. Simultaneous determination of 24 free amino acids in MGC803 cells by hydrophilic interaction liquid chromatography with tandem mass spectrometry. *J. Chromatogr. B* **2019**, *1132*, 121792. [CrossRef]
30. Xu, L.W.; Zha, A.D.; Xiong, X.; Sun, D.H. Determination of succinic acid and lactic acid in pigs' serum, intestinal contents, and meat by ultrahigh-performance liquid chromatography-tandem mass spectrometry. *Rapid Commun. Mass. Spectrom.* **2024**, *38*, e9769. [CrossRef]
31. Wang, X.; Wang, S.; Yi, J.K.; Li, Y.S.; Liu, J.N.; Wang, J.; Xi, J.H. Three host plant volatiles, hexanal, lauric acid, and tetradecane, are Detected by an antenna-biased expressed odorant receptor 27 in the Dark Black Chafer *Holotrichia parallela*. *J. Agric. Food Chem.* **2020**, *68*, 7316–7323. [CrossRef]

Disclaimer/Publisher's Note: The statements, opinions and data contained in all publications are solely those of the individual author(s) and contributor(s) and not of MDPI and/or the editor(s). MDPI and/or the editor(s) disclaim responsibility for any injury to people or property resulting from any ideas, methods, instructions or products referred to in the content.